Journal of Radiotherapy in Practice

Journal of Radiotherapy in Practice (2016)
15, 392–401 © Cambridge University Press 2016
doi:10.1017/S1460396916000340

Technical Note

Study of unflattened photon beams shaped by multileaf collimator using BEAMnrc code

Ankit kajaria[1], Neeraj Sharma[1], Shiru Sharma[1], Satyajit Pradhan[2], Abhijit Mandal[2], Lalit M. Aggarwal[2]

[1]*School of Biomedical Engineering, Indian Institute of Technology (BHU) Varanasi, Varanasi, Uttar Pradesh, India*
[2]*Department of Radiotherapy and Radiation Medicine, Institute of Medical Science (BHU) Varanasi, Varanasi, Uttar Pradesh, India*

(Received 6 June 2016; revised 17 July 2016; accepted 21 July 2016)

Abstract

Purpose: In our study basic dosimetric properties of a flattening filter free 6 MV photon beam shaped by multileaf collimators (MLC) is examined using the Monte Carlo (MC) method.

Methods and Materials: BEAMnrc code was used to make a MC simulation model for 6 MV photon beam based on Varian Clinic 600 unique performance linac, operated with and without a flattening filter in beam line. Dosimetric features including central axis depth dose, beam profiles, photon and electron spectra were calculated and compared for flattened and unflattened cases.

Results: Dosimetric field size and penumbra were found to be smaller for unflattened beam, and the decrease in field size was less for MLC shaped in comparison with jaw-shaped unflattened beam. Increase in dose rate of >2·4 times was observed for unflattened beam indicating a shorter beam delivery time for treatment. MLC leakage was found to decrease significantly when the flattening filter was removed from the beam line. The total scatter factor showed slower deviation with field sizes for unflattened beam indicating a reduced head scatter.

Conclusions: Our study demonstrated that improved accelerator characteristics can be achieved by removing flattening filter from beam line.

Keywords: accelerator characteristics; Monte Carlo simulation; multileaf collimator; unflattened photon beam

INTRODUCTION

Introduction of flattening filter free beams to clinical practice has generated substantial interest in radiotherapy due to the advantages of unflattened beams over flattened beams. Studies have shown that removal of the flattening filter with its associated attenuation from X-ray beam path increases dose rate.[1] The other potential advantages are substantial reduction in head scatter, as the flattening filter is the major source of scattered photons. Improved dosimetry characteristics of

Correspondence to: Ankit kajaria, School of Biomedical Engineering, Indian Institute of Technology (BHU) Varanasi, Varanasi, Uttar Pradesh, India. Tel: 917607066152; E-mail: akajaria.rs.bme12@itbhu.ac.in

unflattened beams are the result of reduced head scatter as variation in output and all field size-dependent parameters with radiation field size decreases.

The Monte Carlo (MC) method has been used extensively to estimate accurate dose distributions for clinical beams. Several studies have been conducted using this method for analysing linac head components and influencing factors on beam characteristics.[2–4] Studies describing the effect of flattening filter on photon energy spectra, absolute absorbed dose and beam profiles have been published.[5] In an earlier MC study, dose rates increase by a factor of 2·31 (6 MV) and 5·45 (18 MV) and out-of-field dose reductions were reported for flattening filter free beams.[6] In a similar study, a significant improvement in out-of-field dose was reported for small field sizes.[7] The effects of multileaf collimators (MLC) on beam characteristics for flattened and unflattened beam were also investigated in previous studies quoting clear advantage of MLC over jaw to define treatment field.[8] The possible advantages of removing the flattening filter from beam line has been outlined by the above studies. Therefore, it is important to investigate these properties for a typical modern accelerator such as the Varian Clinic 600 unique performance. Our study reports on depth-dose dependencies, lateral profiles, total scatter factors, MLC leakage and various fluence spectra of a conventional accelerator and a flattening filter-free system.

MATERIAL AND METHODS

Simulation model for 6 MV Varian Linac

Simulation model of Varian Clinic 600 unique performance was developed using MC code system BEAMnrc[9,10] in our study. To derive the best estimates for the mean energy and full width at half maximum (FWHM) of the electron beam incident on the target, MC simulations for monoenergetic beams ranging from 5·5 to 6·2 MeV with FWHM varied from 0·15 to 0·25 cm were performed to find the best match with percentage depth dose (PDD) and profiles measurements. A monoenergetic source with kinetic energy of the beam 5·7 MeV and FWHM for the X and Y directions of 0·2 cm was found to give best agreement with measured data. Geometry and materials used to build the MC simulation model of the linear accelerator were based on machine specifications as provided by the manufacturer Varian Medical Systems. The linac was structured in the following order: a target slab of tungsten and copper, primary collimator (tungsten), flattening filter, ion chamber, mirror, jaws (tungsten) and finally the option for 120 leaf Varian Millennium™ Multileaf Collimator. All materials used in the MC simulation were extracted from the 700 ICRU PEGS4 (pre-processor for Electron Gamma Shower) cross-section data available in BEAMnrc, and met the specifications for the linac as provided by the manufacturer.

Different stages of simulation for 6 MV photon beam produced by Varian Linac using principal features of the BEAMnrc-DOSXYZnrc code[11,12] are shown in Figure 1. In the simulation of the full accelerator unit we have split the calculation into three steps in order to save time. In the first step, which takes the most computing time, $1{\cdot}5 \times 10^8$ initial histories are initiated and a monoenergetic electron beam source of kinetic energy of 5·7 MeV with FWHM for the X and Y

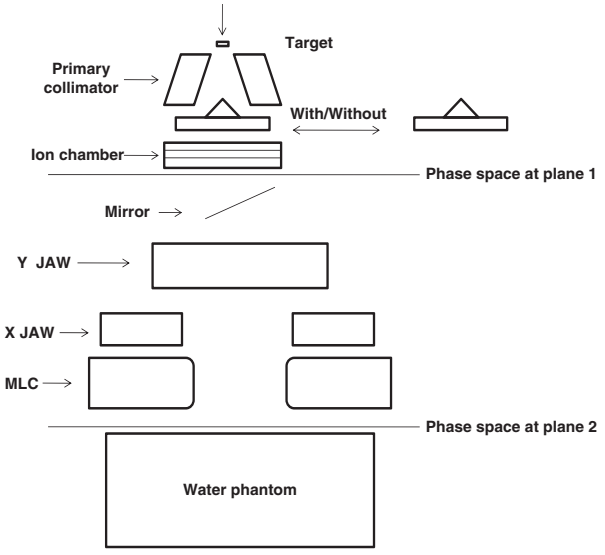

Figure 1. Simulation model for 6 MV Varian Linac separated into three parts, treatment head fixed opening part up to plain one, variable opening part between plain one and plain two and dose calculation inside water phantom in third step.
Abbreviations: MLC, multileaf collimators.

https://doi.org/10.1017/S1460396916000340 Published online by Cambridge University Press

directions of 0·2 cm was incident on the target. The primary collimator, flattening filter and ion chamber are included in this step. The output of this step is a phase space file at plain one as shown in Figure 1, having information of energy, position, direction, charge and history variable for every particle exiting downstream from the end of ion chamber. As the source and primary collimator have fixed openings, it is possible to use this phase space data for the simulation of different field sizes. This large set of particles produced in first step is used repeatedly as the input to the next step of simulation. The second step of the calculation simulates the passage of the particles through the mirror, adjustable collimator, MLC and air slab to a plane at source to surface distance (SSD) 100 cm from target. We simulate different openings of jaw as well as MLC to get field sizes from 5×5 to $20 \times 20\,cm^2$ at an SSD equal to 100 cm. For the latter case, in MLC-defined field sizes the projected jaw setting was 5 cm larger than that of MLC. The output of this step is a phase space file at plain two as shown in Figure 1, having information of energy, position, direction, charge and history variable for every particle reaching the plain at SSD 100 cm from target. The data analysis program BEAMDP[13] is used to analyse the phase space data files to extract the various types of spectra of all particles reaching the plane at SSD 100 cm.

In the third step of the simulation, the phase space files for field sizes of 5×5 to $20 \times 20\,cm^2$ at an SSD of 100 cm which were obtained at the end of second step are reused by the DOSXYZnrc code as an input for dose calculations in a water phantom as shown in Figure 1. We transport the particles through a water phantom of dimension $30 \times 30 \times 30\,cm^3$ with voxels size of $0{\cdot}25 \times 0{\cdot}25 \times 0{\cdot}25\,cm^3$. In the simulation of 'unfiltered' 6 MV photon beam, all three steps of simulation are the same expect in the first step where the flattening filter is being removed from the beam line. A comprehensive set of dosimetric data for 6 MV filtered photon beams where acquired using a three-dimensional (3D) phantom, Blue phontom[2] IBA Dosimetry GmbH and OmniPro-Accept 7 data acquisition software. All the measurements were performed with a Scanditronix/Wellhofer compact ionisation chamber CC13, in the water phantom.

Unflattened beams profiles show much different behaviour from the standard flattened beams and central axis normalisation method cannot be used to describe them. In order to describe the profiles of unflattened beams a normalisation method was proposed by Fogliata et al.[14]. In this method unflattened beams are renormalised to the dose level of a point located in the profile's shoulder of the corresponding flattened beam. This point is located in a region where the two profiles present similar shapes, before the unflattened beam starts to increase in dose towards the beam central axis. In the present work, this renormalisation method was used for calculating following parameters of unflattened beam. The definitions of these parameters which are useful in the characterisation of unflattened beam profiles are summarised here, whereas details can be found in the original study.

Dosimetric field size: The distance between the 50% dose levels in the normalised unflattened beam profiles.

Penumbra: The distance between the 20 and 80% dose levels in the normalised unflattened beam profiles.

RESULTS

Validation of MC simulation model for flattened beam with measurements

In order to validate our simulation model, lateral beam profiles for filtered 6 MV photon beam were calculated for 5×5 to $20 \times 20\,cm^2$ field sizes at 1·5, 5 and 10 cm depths. The measured and calculated lateral dose profiles were normalised to unity on the central axis for comparison. Figure 2 shows the comparison of MC calculations to measured data for a field size of 20×20 and $10 \times 10\,cm^2$ at depth of 10 cm. The lateral field size at the 50% dose level (X_{50}) and penumbra widths, P_{90-10} and P_{80-20} (calculated from the 90% level to the 10% level and from 80 to 20%) were calculated using MC simulation and the results of the comparisons are summarised in Table 1.The differences between the measurement and the simulation results in lateral field size at the 50% dose level, X_{50}, was found to be less than 1 mm.

https://doi.org/10.1017/S1460396916000340 Published online by Cambridge University Press

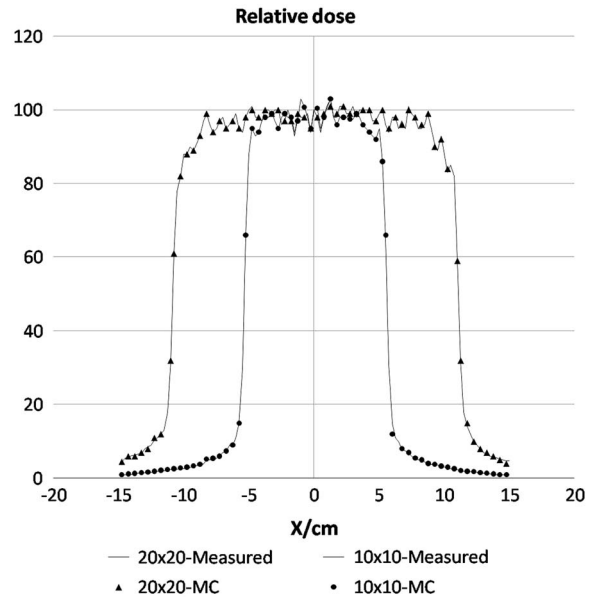

Figure 2. A comparison of measured and calculated beam profiles of the 6 MV photon beam at a depth of 10 cm for 20 × 20 and 10 × 10 cm² field sizes.
Abbreviations: MC, Monte Carlo.

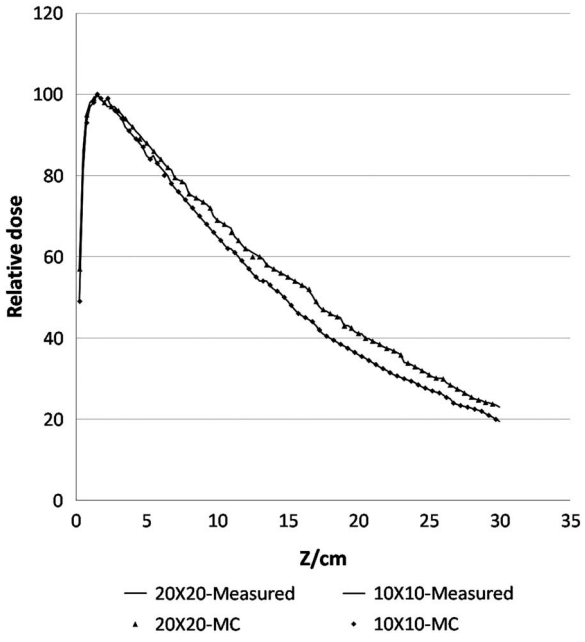

Figure 3. A comparison of measured and calculated depth doses curves of the 6MV photon beam For 20 × 20 and 10 × 10 cm² field sizes.
Abbreviations: MC, Monte Carlo.

Table 1. *Comparison of measured and calculated lateral dose profiles at 10 cm depth*

A (cm^2)	ΔX_{50}	ΔP_{80-20}	ΔP_{90-10}
5 × 5	0·10	1·5	0·8
10 × 10	0·50	1·52	1·0
15 × 15	0·40	1·2	2·0
20 × 20	0·50	1·0	2·2

Abbreviations: A, field size; ΔX_{50}, lateral difference measured at the 50% dose point in the penumbra (mm); ΔP_{90-10}, difference in width of the penumbra measured from the 90% point to 10% dose point (mm); ΔP_{80-20}, difference in width of the penumbra measured from 80 to 20% dose point (mm).

Table 2. *Comparison of calculated and measured central-axis depth-dose profiles at various field sizes*

A (cm^2)	d_{max} (Simulated)	d_{max} (Measured)	ΔD_{max}
5 × 5	1·5	1·56	0·2
10 × 10	1·5	1·52	0·17
15 × 15	1·48	1·5	0·13
20 × 20	1·38	1·40	0·10

Abbreviations: A, field size; d_{max}, location of the maximum dose (cm); ΔD_{max}, relative dose difference between the measurement and the calculations at d_{max}.

Depth-dose curves for filtered 6 MV photon beam for field size 5 × 5 to 20 × 20 cm^2 were calculated in an axis cylinder of radius 1 cm using MC simulation and compare with measured data for the validation of simulation model. The calculated central axis depth-dose curves were normalised to unity at the depth, d_{max}, of the maximum dose deposition, D_{max}. Both results measured and calculated, could then be compared with respect to the relative value of the maximum dose D_{max} and the corresponding depth d_{max}. Figure 3 shows the comparison between the calculated depth-dose distributions and measurements for two different field sizes studied in this work. The comparison shows that the calculated and measured data agree within 1% of local relative dose, and 1 mm in depth at all depths and field sizes which are summarised in Table 2.

Comparison of unflattened and flattened beam characteristics

Profile comparison

Lateral profiles of unflattened and flattened beams for different field sizes were calculated at 1·5, 5 and 10 cm depth inside a water phantom. The comparison of unflattened and flattened beams for field sizes 10 × 10 and 20 × 20 cm^2 at a depth of

https://doi.org/10.1017/S1460396916000340 Published online by Cambridge University Press

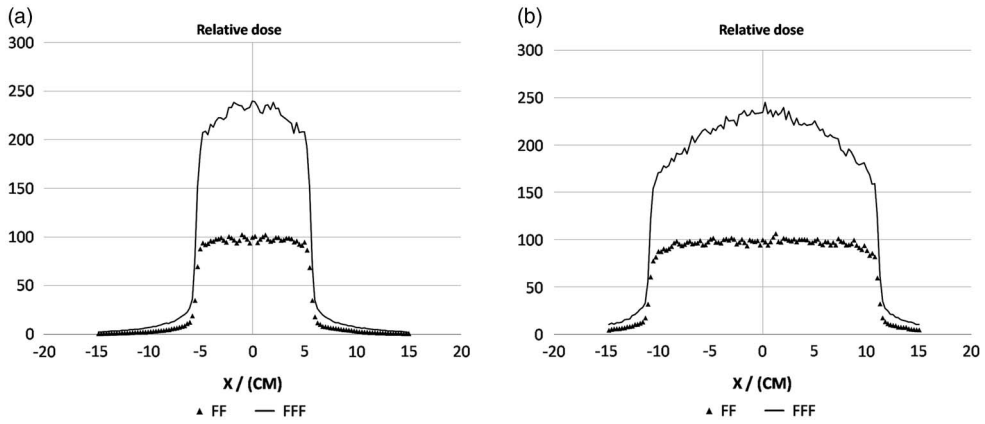

Figure 4. Lateral profile comparison for 6 MV unflattened photon beams with flattened beam at 10 cm depth for field size (a) 10 × 10 cm^2 (b) 20 × 20 cm^2.
Abbreviations: FF and FFF, flattened and unflattened beams, respectively.

Table 3. *Calculated profile parameters for unflattened 6 MV photon beam for jaw and multileaf collimators (MLC) defined field sizes*

	Field size: 5 × 5 cm^2		Field size: 10 × 10 cm^2		Field size: 20 × 20 cm^2	
	Jaw define field	**MLC define field**	**Jaw define field**	**MLC define field**	**Jaw define field**	**MLC define field**
MC-calculated field size (cm)	$d = d_{max}$ 5·06 d = 10 cm 5·63	$d = d_{max}$ 5·12 $d = d_{max}$ 5·75	$d = d_{max}$ 10·10 d = 10 cm 11·06	$d = d_{max}$ 10·25 d = 10 cm 11·20	$d = d_{max}$ 20·12 d = 10 cm 22·08	$d = d_{max}$ 20·25 d = 10 cm 22·25
MC-calculated penumbra (cm)	$d = d_{max}$ 0·20 d = 10 cm 0·43	$d = d_{max}$ 0·23 d = 10 cm 0·47	$d = d_{max}$ 0·23 d = 10 cm 0·53	$d = d_{max}$ 0·31 d = 10 cm 0·59	$d = d_{max}$ 0·27 d = 10 cm 0·76	$d = d_{max}$ 0·35 d = 10 cm 0·89

Notes: Data were calculated at source to surface distance = 100 cm.
Abbreviations: d, depth inside water phantom, MC, Monte Carlo.

10 cm is shown in Figure 4. Extremely different dose profiles compared with the flattened beams are presented by unflattened beams: a forward-peaked profile of unflattened beam on central axis is characteristically seen in all field sizes. Hence, broadly used profile parameters for defining flattened beam would need modification in order to adapt their interpretation to unflattened beams, whereas keeping the main concepts valid for both unflattened and flattened cases. In our study, we used the normalisation method described by Fogliata et al.[14] to calculate the characteristics of unflattened photon beams shaped by jaw and MLC-defined field in terms of field size and penumbra at two different depths for three field sizes which are presented in Table 3.

Analysis of spectra

Photon fluences spectra

Central axis photon spectra as a function of energy (number of photons per MeV per incident electron on the target) is calculated and presented in Figure 5. Photons originating from the target pass through the collimating system on their way to the scoring plain at an SSD 100 cm. Scoring plain is an annular region around the central axis with radius $0 < r < 2{\cdot}25$ cm. The range of possible energy of photons is divided into interval (bin) of 0·25 MeV. The number of photons within each energy interval, crossing the scoring plain is being recorded for flattened and unflattened case separately. The precision of calculated central-axis photon spectra for all the field size used in the dose calculations is high and uncertainty in each 0·25 MeV wide bin is usually between 1 and 5%, except for the high-energy end of the spectra. There is a noticeable increase observed in the photon fluence when the flattening filter is removed from the beam line.

Average energy distribution

Photon average energies distribution as a function of off-axis distance calculated for field size 20 × 20 cm^2 at 100 cm SSD show considerable

https://doi.org/10.1017/S1460396916000340 Published online by Cambridge University Press

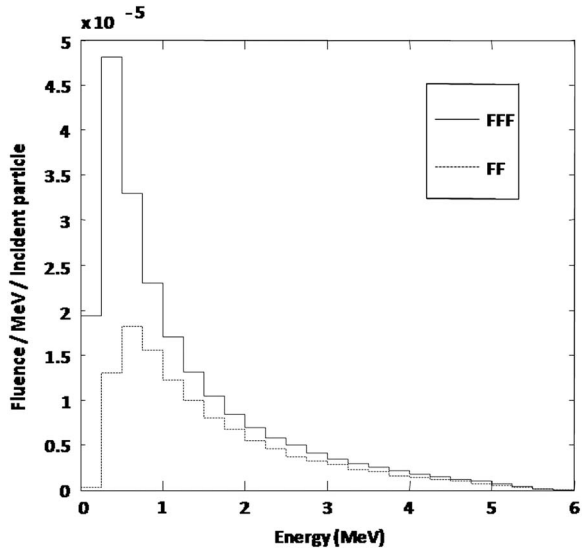

Figure 5. Photon fluences per initial electron on the target, at the top of the water phantom as a function of energy (MeV) for $20 \times 20\,cm^2$ field size calculated for with/without a flattening filter in beam line.
Abbreviations: FF and FFF denotes flattened and unflattened beams, respectively.

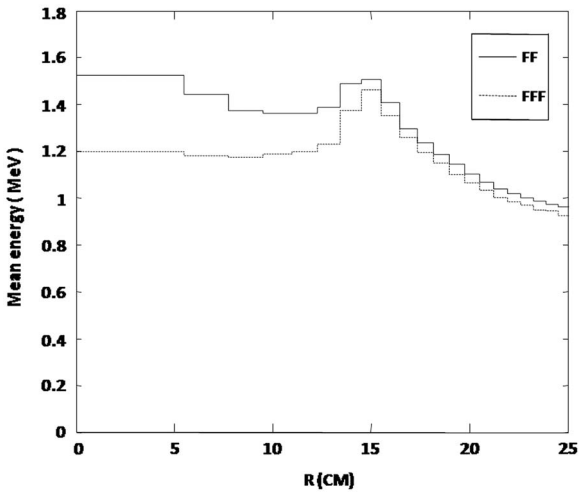

Figure 6. Photon average energy distribution of the filtered and unfiltered 6 MV beams as a function of off-axis distance for $20 \times 20\,cm^2$ field size and 100 cm source to surface distance.
Abbreviations: FF and FFF, flattened and unflattened beams, respectively.

difference for flattened and unflattened cases which is presented in Figure 6. It is observed from above distribution that mean photon energy for flattened beam to have a value at central axis 1·5 MeV and decrease to 1·2 MeV at off-axis distance of 20 cm which verifies the beam hardening effect produced by the flattening filter[5] for the filtered beam. For the unflattened beam, the mean energy of spectra was not changed significantly with increasing off-axis distance and it was, respectively, decreased from 1·25 MeV on central axis to 1·19 MeV at 20 cm off-axis distance for $20 \times 20\,cm^2$ field size.

Contaminant electron fluence spectra
Increase in electron fluence can cause the risk of placing ion chamber used for the measurement outside the range of its reliable operation. Also, it is a major component of elevated skin dose delivered to patient. Figure 7 shows the calculated fluence spectra for contaminant electrons calculated for central axis with radius $0 < r < 2{\cdot}25$ cm and energy bin of 0·25 MeV at 100 cm SSD for with/without flattening filter case separately. In our study it is found that the number of electron reaching the phantom surface increases with removing the flattening filter from the beam line. The averaged value of electron fluence spectra calculated for without flattening filter case is found to be 1·3 times greater than its value for with flattening filter case for field size $20 \times 20\,cm^2$.

Depth-dose analysis
Absolute dose. For comparison purposes absolute absorbed dose per initial electron on target were calculated for flattened and unflattened beam at two reference depths of 1·5 and 10 cm. The ratio of absolute depth doses for flattening filter free to standard flattened beams were calculated and are presented in Table 4. Significant increase in absorbed dose was observed by removing flattening filter, indicating an increase in dose rate for unflattened beam. However, the increase in dose rate is decreased with increasing depth.

Percentage depth-dose characteristics

Percentage depth-dose characteristics
Absolute depth-dose values were used to calculate PDD characteristics curves. It can be seen from Figure 8 that unflattened beam show slightly lower PDDs values in comparison with the standard beam for all field sizes. Difference in the PDDs between the two cases is evident at deeper

https://doi.org/10.1017/S1460396916000340 Published online by Cambridge University Press

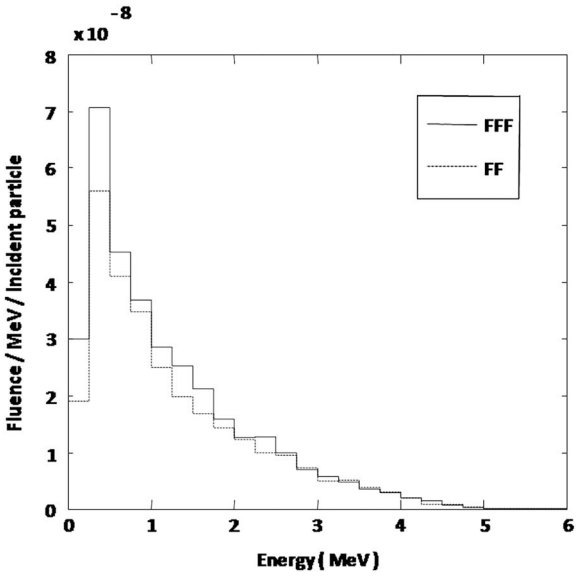

Figure 7. Electron fluences per initial electron on target, at the top of the water phantom as a function of energy for 20 × 20 cm² field size calculated for with/without a flattening filter in beam line. Abbreviations: FF and FFF, flattened and unflattened beams, respectively.

Table 4. *Ratios of absolute depth doses for flattening filter free to flattened beams at two reference depths for different field sizes*

A (cm²)	$\left(\frac{D_{FFF}}{D_{FF}}\right)$ at d = 1·5	$\left(\frac{D_{FFF}}{D_{FF}}\right)$ at d = 10
5 × 5	2·49	2·42
10 × 10	2·47	2·45
20 × 20	2·44	2·40

Notes: Absorbed dose calculated without the flattening filter in the beam line is denoted as D_{FFF} (flattening filter free) and with filter in beam line is denoted as D_{FF}.
Abbreviations: A, field size; d, depth inside water phantom.

depths and is increased with depth for10 × 10 and 20 × 20 cm² field sizes. This difference is validated by calculating two parameters which are reported in Table 5, namely, the relative dose at a depth of 10 and 20 cm (D_{10}, D_{20}).

MLC leakage

MLC leakage is an important parameter needed for the commissioning of a treatment-planning system. We calculated the MLC leakage as a function of field size for the unflattened profile in our study and is presented in Table 6. MLC leakage represents the dose on the central beam axis with MLC-blocked fields normalised by the dose of open fields of the same field size at 1·5 cm depth for SSD 100 cm. Open MLC field are defined as the MLC leaves are withdrawn underneath the jaws so as to not intercept the beam, the field size is defined by the treatment jaws. MLC-blocked fields define a field in which the MLC leaves are configured to fully block the open field produced by the jaw. To ensured that the jaws blocked the rounded tips of the leaves completely in MLC-blocked fields the leaves of MLC were positioned asymmetrically with respect to the central axis and there projected offset at isocenter was 8·0 cm.

Scatter function

The total scatter factor, S_{CP} is defined as 'the dose rate at a reference depth for a given field size divided by the dose rate at the same point and depth for the reference field size (10 × 10 cm²)'. It was measured at SSD = 100 cm and a depth equal to d_{max} of a 10 × 10 cm² field for different field sizes. The data for with/without flattening filter case are presented in Table 7.

The unflattened beams is found to have less value of S_{CP} for lager field sizes in comparison with flattened beams which indicate a reduced head scatter in unflattened beams compared with the standard flattened beam.

DISCUSSION

In present study, we attempt to use new parameters defined in an earlier study by Fogliata et al.[14] to describe the characteristics of unflattened beam shaped by jaw and MLC. It was observed that the dosimetric field size is slightly smaller for unflattened beam compared with flattened beam, however the amount of reduction in field size was less for MLC shaped in comparison with jaw-shaped unflattened beam. The maximum difference in MLC and jaw-shaped unflattened beam is 1·7 mm for 20 × 20 cm² field size at 10 cm depth and it is even less for smaller field sizes. The beam penumbra for unflattened case was also found to be smaller than that of flattened case. However, difference in penumbra values for unflattened beam shaped by MLC and jaw were small with maximum value of 1·3 mm. This difference may

https://doi.org/10.1017/S1460396916000340 Published online by Cambridge University Press

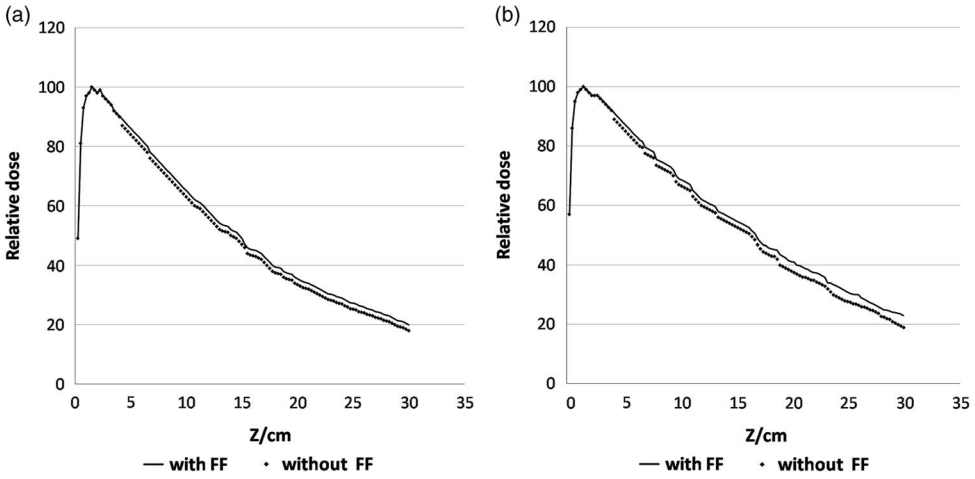

Figure 8. Comparison of relative depth-dose curves calculated for with and without flattening filter for 6 MV photon beams for different field sizes: (a) 10 × 10 cm^2 (b) 20 × 20 cm^2.
Abbreviations: FF and FFF, flattened and unflattened beams, respectively.

Table 5. *Comparison of relative depth doses for flattening filter free to standard flattened beams at two reference depths for different field sizes*

A (cm^2)	D_{10}		D_{20}	
	With FF	Without FF	With FF	Without FF
5 × 5	62·43	59·40	33·26	30·84
10 × 10	66·70	63·80	37·80	34·34
20 × 20	71·65	68·96	40·98	37·55

Abbreviations: *A*, field size; D_{10} and D_{20}, relative depth dose at 10 and 20 cm depth; FF = flattening filter.

Table 6. *Calculated multileaf collimators (MLC) leakage for 6 MV photon beam deliver with or without flattening filter in beam line for different field sizes*

Field size (cm^2)	MLC linkage	
	With flattening filter	Without flattening filter
5 × 5	–	1·10
10 × 10	1·40	1·23
20 × 20	–	1·32

Notes: Calculations were made at 1·5 cm depth and source to surface distance 100 cm.

not appear large, but are important in modern radiation treatments. These characteristics of unflattened beam can be described as the flattening filter elevates relative fluence of primary photons propagating off-axis and reduced amount of head scatter present in unflattened beams. Unflattened beam characteristics were found to be comparable with flattened beam within a few centimetres from the central axis. Therefore unflattened beams are unlikely to present a problem for treatments with small fields, moreover the treatments can also profit from an increased dose rate.

Average energy distribution as a function of off-axis distance and central axis photon fluence spectra as a function of energy for flattened and unflattened beams are being calculated in our study. An increase of two-fold was observed in fluence of photon on central axis averaged over the total surface of the top of water phantom with removing flattening filter. However, energy spectrum became softer and the average energy of photon energy spectrum on central axis was decreased from 1·5 to 1·25 MeV by removing flattening filter at the top of water phantom for 20 × 20 cm^2 field size at 100 cm SSD. Also the average energy of photon for flattened beam was found to decrease more with increasing off-axis distance in comparison with unflattened beam. The differential attenuation caused by flattening filter with increasing distance from central axis of beam is the possible explanation for this behaviour. The thick central part of the flattening filter attenuate more low-energy photons, but as

https://doi.org/10.1017/S1460396916000340 Published online by Cambridge University Press

Table 7. *Total scatter factor (S_{CP}) of 6 MV photon beams measured for with/without a flattening filter cases*

Field size (cm^2)	S_{CP} (MLC shaped with flattening filter)	S_{CP} (jaw shaped without flattening filter)	S_{CP} (MLC shaped without flattening filter)
5 × 5	0·967	0·97	0·98
10 × 10	1	1	1
15 × 15	1·021	1·012	1·010
20 × 20	1·054	1·027	1·018

Notes: The S_{CP} was measured at source to surface distance = 100 cm, and at the depth of maximum dose d_{max} of a $10 \times 10\ cm^2$ field size.
Abbreviations: MLC, multileaf collimators.

the off-axis distance increases, more low-energy photons are allowed to penetrate the thin lateral part of the flattening filter and they contribute to the photon energy spectrum, thus the mean energy of spectrum is decreased. Therefore for unflattened beam no such significant change in mean energy of spectrum was observed with increasing off-axis distance and it was, respectively, decreased from 1·25 MeV on central axis to 1·19 MeV at 20 cm off-axis distance for $20 \times 20\ cm^2$ field size.

Flattening filter is a major source of scattering and absorption of a large fraction of primary photons in conventional clinical linear accelerators. Due to this reason, it is the main cause of increase in beam-on time and out-of-field exposure to patients. Thus removing the filter from the beam line should result in substantial increase in dose rate and therefore a decrease in beam-on time should be achieved when radiation treatment is delivered. To validate this effect, absolute absorbed dose per initial electron were calculated for flattened and unflattened beam at two different depths for different field sizes. The ratios of absolute depth doses calculated in our study for unflattened beam to standard flattened beams for field size $10 \times 10\ cm^2$, at 10 cm depth for an SSD equal to 100 cm was found to be 2·45 demonstrating the potential higher dose rate deliver by the unflattened beam. Unflattened beam is found to have slightly lower PDDs value compared with the standard beam for all field sizes. Difference in the PDDs of flattened and unflattened beams are apparent at deeper depths and are increased with increase in depth for all the field sizes.

MLC leakage was calculated for flattened and unflattened beam in our study. It was observed that there is a substantial decrease in MLC leakage when the flattening filter was removed from the beam line, as for $10 \times 10\ cm^2$ field size its value was 1·4 which decrease to 1·23 with filter removed from the beam line. The average energy difference on the central axis is considered to be the major reason for this decrease. As the filter is removed from the beam line, the average energy of photon beam decreases causing more attenuation of the photon beam by MLC. The analysis of total scatter factor, S_{CP} calculated for unflattened and flattened beam has shown that S_{CP} increases more slowly with increasing field size for unflattened beam in comparison to that of flattened beam. In addition, the amount of variation in S_{CP} was even less for MLC shaped in comparison with jaw-shaped unflattened beam. The forward-peaked profile of unflattened beam produces less S_{CP} because of the reduced off-axis intensity. The unflattened beam has greatly reduced fluence off-axis, hence, less secondary head scatter is created, which is directed in towards the central axis. This is why as the measured field size increases, the expected increase in S_{CP} for unflattened beams is not seen which is found with the flattened ones.

CONCLUSION

A MC simulation model of 6 MV photon beam from Varian Clinic 600 unique performance accelerator was developed and benchmarked against measurements. Basic dosimetric properties of photon beam generated by the accelerator with the flattening filter removed from beam line were investigated with this model. New definitions for some dosimetric parameters such as field size and penumbra suggested by Fogliata et al.[14] were used to describe the unflattened beam profiles. We found that the dosimetric field size and penumbra is slightly smaller for unflattened beam and the decrease in field size was less for MLC shaped in comparison with jaw-shaped unflattened beam. Less variation in total scatter factor, S_{CP} with field sizes was observed which indicate that removing the filter from beam line can reduce head scatter and therefore doses to normal tissues and organs.

https://doi.org/10.1017/S1460396916000340 Published online by Cambridge University Press

A considerable decrease in MLC leakage was observed for unflattened beam which is due to the difference in average energy on the central axis for the two cases. An increase of >2·4 times was observed in dose rate of unflattened beam which suggest that higher central-axis dose rates and shorter beam delivery time for treatments can be achieved by removing the flattening filter from beam line.

Acknowledgements

The authors thank Varian Medical Systems for providing us with the specifications needed for linac simulations.

Financial support

This research received no specific grant from any funding agency, commercial or not-for-profit sectors.

Conflicts of Interest

The authors declare that they have no conflicts of interests.

Ethical Standards

'This article does not contain any studies with human participants or animals performed by any of the authors'.

References

1. Fu W, Dai J, Hu Y, Han D, Song Y. Delivery time comparison for intensity-modulated radiation therapy with/without flattening filter: a planning study. Phys Med Biol 2004; 49 (8): 1535.
2. Verhaegen F, Seuntjens J. Monte Carlo modelling of external radiotherapy photon beams. Phys Med Biol 2003; 48 (21): R107.
3. Sheikh-Bagheri D, Rogers DW. Monte Carlo calculation of nine megavoltage photon beam spectra using the BEAM code. Med Phys 2002; 29 (3): 391–402.
4. Mesbahi A, Reilly AJ, Thwaites DI. Development and commissioning of a Monte Carlo photon beam model for Varian Clinac 2100EX linear accelerator. Appl Radiat Isot 2006; 64 (6): 656–662.
5. Lee PC. Monte Carlo simulations of the differential beam hardening effect of a flattening filter on a therapeutic X-ray beam. Med Phys 1997; 24 (9): 1485–1489.
6. Vassiliev ON, Titt U, Kry SF, Pönisch F, Gillin MT, Mohan R. Monte Carlo study of photon fields from a flattening filter-free clinical accelerator. Med Phys 2006; 33 (4): 820–827.
7. Titt U, Vassiliev ON, Pönisch F, Dong L, Liu H, Mohan R. A flattening filter free photon treatment concept evaluation with Monte Carlo. Med Phys 2006; 33 (6): 1595–1602.
8. Pönisch F, Titt U, Vassiliev ON, Kry SF, Mohan R. Properties of unflattened photon beams shaped by a multileaf collimator. Med Phys 2006; 33 (6): 1738–1746.
9. Rogers DW, Faddegon BA, Ding GX, Ma CM, We J, Mackie TR. BEAM: a Monte Carlo code to simulate radiotherapy treatment units. Med Phys 1995; 22 (5): 503–524.
10. Rogers DW, Walters B, Kawrakow I. BEAMnrc Users Manual, NRC Report PIRS 509(A)revH. Ionizing Radiation Standards. Ottawa, ON: NRC, 2004/2005.
11. Kawrakow I, Walters BR. Efficient photon beam dose calculations using DOSXYZnrc with BEAMnrc. Med Phys 2006; 33 (8): 3046–3056.
12. Walters B, Kawrakow I, Rogers DW. DOSXYZnrc Users Manual. NRC Report PIRS. Ottawa, ON: NRC, 2005.
13. Ma CM, Rogers DW. BEAMDP Users Manual. NRC Report PIRS-0509 (D). Ottawa, ON: NRC, 1995.
14. Fogliata A, Garcia R, Knöös T et al. Definition of parameters for quality assurance of flattening filter free (FFF) photon beams in radiation therapy. Med Phys 2012; 39 (10): 6455–6464.